

Nickel(II) Thiolate Complex with Carbon Monoxide and Its Fe(II) Analog: Synthetic Models for CO Adducts of Nickel–Iron-Containing Enzymes

Dao Hinh Nguyen, Hua-Fen Hsu, Michelle Millar,* and Stephen A. Koch*

Department of Chemistry
State University of New York at Stony Brook
Stony Brook, New York 11794-3400

Catalina Achim, Emile L. Bominaar, and Eckard Münck*

Department of Chemistry
Carnegie Mellon University
Pittsburgh, Pennsylvania 15213

Received June 11, 1996

Carbon monoxide is a substrate for two distinct reactions catalyzed by the iron–nickel-containing enzyme carbon monoxide dehydrogenase (CODH).^{1,2} The oxidation of CO to CO₂ occurs at one site (center C) while CO combines with a methyl group to form an acetyl group at the second site (center A). Both of these reactions occur at reaction centers that involve closely coupled Ni and Fe centers. Recent vibrational studies have suggested that the CO is bound to iron and not to nickel at center A and that nickel is involved in the CO oxidation at center C.² CO has also been used as an inhibitor and a spectroscopic marker for the nickel–iron-containing hydrogenase enzymes.³ Two distinct CO adducts of the nickel–iron hydrogenases have been spectroscopically detected: (1) an EPR active form which displays hyperfine couplings indicating direct Ni–CO coordination⁴ and (2) a postulated Ni(II)–CO form which displays a CO stretch at 2060 cm⁻¹.⁵ The recent X-ray structure determination of the nickel–iron-containing hydrogenase revealed that the nickel is bridged by two cysteines to a second metal which is presumably iron.⁶ In both the hydrogenase and CODH enzymes substantial cysteine coordination to the metal centers has been established or suggested.^{6,7} We report the synthesis and characterization of the first example of a nickel(II) thiolate–CO complex and its Fe(II) analog, which is an unprecedented paramagnetic Fe(II)–CO complex.

Nickel complexes of the tripod phosphine trithiolate ligand tris(2-thiophenyl)phosphine (PS3) and its sterically hindered analog tris(3-phenyl-2-thiophenyl)phosphine (PS3*) have been recently investigated.⁸ The reaction of Ni(acac)₂ with Li₃[PS3*] in MeOH generates a yellow-brown solution which changes to a deep green color upon the addition of carbon monoxide.

(1) (a) Ragsdale, S. W. *Crit. Rev. Biochem. Mol. Biol.* **1991**, *26*, 261–300. (b) Xia, J.; Lindahl, P. A. *J. Am. Chem. Soc.* **1996**, *118*, 483–484, and reference therein.

(2) (a) Qiu, D.; Kumar, M.; Ragsdale, S. W.; Spiro, T. G. *Science (Washington, D. C.)* **1994**, *264*, 817–819. (b) Kumar, M.; Qiu, D.; Spiro, T. G.; Ragsdale, S. W. *Science (Washington, D. C.)* **1995**, *270*, 628–630. (c) Qiu, D.; Kumar, M.; Ragsdale, S. W.; Spiro, T. G. *J. Am. Chem. Soc.* **1995**, *117*, 2653–2654. (d) Hu, Z.; Spangler, N. J.; Anderson, M. E.; Xia, J.; Ludden, P. W.; Lindahl, P. A.; Münck, E. *J. Am. Chem. Soc.* **1996**, *118*, 830–845.

(3) Albracht, S. P. J. *Biochim. Biophys. Acta* **1994**, *1188*, 167–204.

(4) van der Zwaan, J. W.; Coremans, J. M. C. C.; Bouwens, E. C. M.; Albracht, S. P. J. *Biochim. Biophys. Acta* **1990**, *1041*, 101–110.

(5) Bagley, K. A.; Van Garderen, C. J.; Chen, M.; Duin, E. C.; Albracht, S. P. J.; Woodruff, W. H. *Biochemistry* **1994**, *33*, 9229–9236. Bagley, K. A.; Duin, E. C.; Roseboom, W.; Albracht, S. P. J.; Woodruff, W. H. *Biochemistry* **1995**, *34*, 5527–5535.

(6) Volbeda, A.; Charon, M.-H.; Piras, C.; Hatchikian, E. C.; Frey, M.; Fontecilla-Camps, J. C. *Nature (London)* **1995**, *373*, 580–587.

(7) Xia, J.; Dong, J.; Wang, S.; Scott, R. A.; Lindahl, P. A. *J. Am. Chem. Soc.* **1995**, *117*, 7065–7070.

(8) (a) Franolic, J. D.; Wang, W. Y.; Millar, M. *J. Am. Chem. Soc.* **1992**, *114*, 6588. (b) Nguyen, D. H.; Millar, M. Submitted for publication.

(9) Electronic spectrum of **1** in DMF (λ , nm (ϵ_M)): 297 (10 300 M⁻¹ cm⁻¹), 368 (6250), 722 (913).

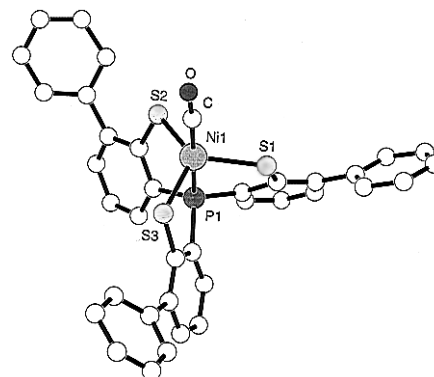


Figure 1. Structural diagram of $[\text{Ni}(\text{PS3}^*)(\text{CO})]^{1-}$ **1**. Selected bond distances (Å) and angles (deg): Ni–S1, 2.352(6); Ni–S2, 2.274(5); Ni–S3, 2.312(6); Ni–C37, 1.75(3); Ni–P1, 2.089(6); C37–O1, 1.15(2); S1–Ni–S2, 122.6(2); S1–Ni–S3, 109.8(2); S2–Ni–S3, 124.2(2); S1–Ni–P1, 82.6(2); S2–Ni–P1, 83.8(2); S3–Ni–P1, 85.1(2); S1–Ni–C37, 98.1(9); S2–Ni–C37, 92.8(8); S3–Ni–C37, 97.9(8); P1–Ni–C37, 176.4(8).

Subsequent addition of $[(n\text{-Bu})_4\text{N}]\text{Br}$ provides crystalline $[(n\text{-Bu})_4\text{N}][\text{Ni}(\text{PS3}^*)(\text{CO})]$ (**1**) in good yield.⁹ $[(n\text{-Bu})_4\text{N}][\text{Ni}(\text{PS3}^*)(\text{CO})]$ was shown to be diamagnetic and to exhibit an IR stretch at 2029 cm⁻¹ assigned to the Ni(II)–CO center.

The X-ray structure of $[(n\text{-Bu})_4\text{N}][\text{Ni}(\text{PS3}^*)(\text{CO})]$ (Figure 1) reveals a distorted trigonal bipyramidal structure with the CO in the axial position *trans* to the phosphorus atom.¹⁰ The three equatorial thiolate ligands show a distortion from rigorous C₃ symmetry with S–Ni–S angles of 122.6(2), 109.8(2), and 124.2(2)° and Ni–S distances of 2.352(6), 2.274(5), and 2.312(6) Å. The Ni center is situated 0.3 Å out of the plane defined by the three S atoms and toward the CO ligand. The Ni(II)–S distance is 0.07 Å longer than the corresponding distances in $[\text{Ni}^{\text{III}}(\text{PS3}^*)(N\text{-methylimidazole})]$, which is consistent with the anticipated difference in metal–sulfur distances of Ni(II)/Ni(III) oxidation levels.^{8b}

$[(n\text{-Bu})_4\text{N}][\text{Ni}(\text{PS3}^*)(\text{CO})]$ is the first example of a structurally characterized Ni–CO complex with thiolate ligands. Nickel(I) thiolate–CO complexes have been generated in solution but have not been isolated.¹¹ It is noted that Ni(II)–CO complexes with any type of ligand are rare.¹² The axial coordination of the CO in **1** contradicts the molecular orbital prediction of a preference for equatorial coordination of π -acid ligands in trigonal bipyramidal d⁸ compounds.¹³ Examples are known for both axial and equatorial coordination of CO in trigonal bipyramidal Ni(II) compounds. In $\text{NiX}_2(\text{CO})(\text{PMe}_3)_2$ (X = Cl, I)^{12a,b} the CO occupies an equatorial position, while in $\text{NiI}_2(\text{CO})(1,1'\text{-bis(dimethylarsine)ferrocene})$ ^{12c} the CO coordinates in the axial position. The axial coordination of CO in the latter compound was rationalized to result from the constraint of the bidentate arsine ligand. Likewise, the coordination of

(10) Crystal data for **1** (NiPS₃NOC₅₃H₆₀): monoclinic, $P2_1/c$ (no. 14), $a = 16.816(4)$ Å, $b = 16.179(2)$ Å, $c = 17.901(4)$ Å, $\beta = 97.94(1)^\circ$, $V = 4823(1)$ Å³, $Z = 4$. A total of 2470 unique reflections with $I > 3\sigma(I)$ were refined to $R = 0.063$ and $R_w = 0.094$.

(11) Yamamura, T.; Sakurai, S.; Arai, H.; Miyamae, H. *J. Chem. Soc., Chem. Commun.* **1993**, 1656. Marganian, C. A.; Vazir, H.; Baidya, N.; Olmstead, M. M.; Mascharak, P. K. *J. Am. Chem. Soc.* **1995**, *117*, 1584–1594.

(12) (a) Saint-Joly, C.; Mari, A.; Gleizes, A.; Dartiguenave, M.; Dartiguenave, Y.; Galy, J. *Inorg. Chem.* **1980**, *19*, 2403–2410. (b) Elbaze, G.; Dahan, F.; Dartiguenave, M.; Dartiguenave, Y. *Inorg. Chim. Acta* **1984**, *85*, L3–L5. (c) Pierpont, C. G.; Eisenberg, R. *Inorg. Chem.* **1972**, *4*, 828–832. (d) Janikowski, S. K.; Radonovich, L. J.; Groshens, T. J.; Klabunde, K. J. *Organometallics* **1985**, *4*, 396–398. (e) Zebrowski, J. P.; Hayashi, R. K.; Dahl, L. F. *J. Am. Chem. Soc.* **1993**, *115*, 1142–1144.

(13) (a) Rossi, A. R.; Hoffmann, R. *Inorg. Chem.* **1975**, *14*, 365–374. (b) Macgregor, S. A.; Lu, Z.; Eisenstein, O.; Crabtree, R. H. *Inorg. Chem.* **1994**, *33*, 3616–3618.

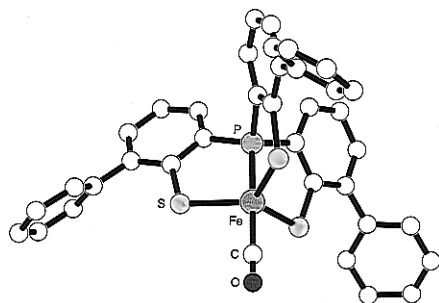


Figure 2. Structural diagram of $[\text{Fe}(\text{PS}_3^*)(\text{CO})]^{1-}$ **2**. Selected bond distances (Å) and angles (deg): Fe–S1, 2.290(4); Fe–P1, 2.165(7); Fe–C13, 1.88(3); S1–Fe–S1', 119.35(3); S1–Fe–P1, 85.4(1); S1–Fe–C13, 94.6(1); P1–Fe–C13, 180.00.

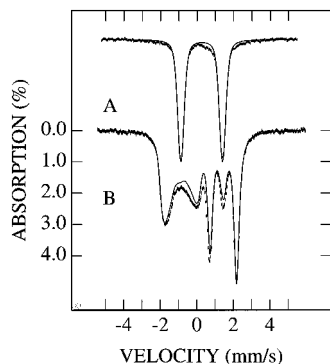


Figure 3. Mössbauer spectra of polycrystalline **2** recorded in zero field at 4.2 K (A) and in a parallel 8.0 T field at 10 K (B). Solid lines are spectral simulations based on eq 1 assuming fast spin relaxation.

the CO in the axial position in **1** may be the result of the structural constraint exerted by the tripod ligand.

The coordination of CO to nickel in **1** is robust. The application of a continuous vacuum to a solution of **1** in DMF does not result in the loss of the CO ligand. This is in contrast to the lability of the CO ligand in some of the previously reported Ni(II)–CO complexes.^{12,13b} However, attempts to oxidize **1** to a Ni(III)–CO species result in loss of CO. Electrochemical studies of **1** indicate an irreversible oxidation at +270 mV (vs SCE) and an irreversible reduction at –400 mV.

The iron analog of **1** is synthesized by the reaction of $\text{FeCl}_2 \cdot 4\text{H}_2\text{O}$ with $\text{Li}_3(\text{PS}_3^*)$ in CH_3CN under a CO atmosphere.¹⁴ $[\text{Et}_4\text{N}][\text{Fe}(\text{PS}_3^*)(\text{CO})]$ (**2**) crystallizes in a cubic space group such that the anion has a crystallographic C_3 axis (Figure 2).¹⁵ The iron is situated 0.19 Å out of the S_3 plane with an Fe–S distance of 2.290(4) Å. The Fe–C distance (1.88(3) Å) is 0.1 Å longer than the corresponding Ni–C distance in **1**. There are numerous examples of Fe(II)–CO complexes including examples with thiolate ligands.¹⁶ The CO stretching frequency (1940 cm^{-1}) of $[\text{Et}_4\text{N}][\text{Fe}(\text{PS}_3^*)(\text{CO})]$ is the same

(14) For **2**, UV–vis in DMF (λ , nm (ϵ_M)) 332 (1.24 $\times 10^4$), 357 (1.18 $\times 10^4$), 524(4.00 $\times 10^3$), 744(5.01 $\times 10^2$); $^1\text{H NMR}$ (DMSO- d_6) δ –29.68 (3H), –5.88 (3H), 1.13 (12H, NCH_2CH_3), 3.15(8H, NCH_2), 7.73–7.55 (12H), 8.85 (3H), 10.26 (3H); CV (1 mM in CH_2Cl_2 with 0.1 M $[\text{NBu}_4][\text{BF}_4]$, Pt electrode, vs SCE) $E_{1/2}(\Delta E_p) = 0.083$ V (67 mV).

(15) Crystal data for **2** ($\text{FePS}_3\text{ONC}_{45}\text{H}_{44}$): cubic, $P2_13$, $a = 15.8730(8)$ Å, $V = 3999.2(2)$ Å³, $Z = 4$. A total of 648 unique reflections with $I > 3\sigma(I)$ were refined to $R = 0.052$ and $R_w = 0.055$. The NEt_4 cation was located on a 3-fold axis and was disordered.

(16) Sellmann, D.; Weiss, R.; Knoch, F.; Dengler, J. *Inorg. Chem.* **1990**, 29, 4107–4114. Sellmann, D.; Brinker, G.; Moll, M.; Herdtweck, E. *J. Organomet. Chem.* **1988**, 327, 403–418. Sellmann, D.; Becker, T.; Knoch, F.; Moll, M. *Inorg. Chim. Acta* **1994**, 219, 75–84.

in solution and in the solid state, indicating that the solid state structure is unchanged in solution. Compound **2** exhibits a reversible oxidation at +0.083 V (vs SCE). However, bulk electrolysis indicates the oxidation is associated with loss of CO.

Carbon monoxide compounds usually have low-spin electronic states. A diamagnetic ground state is not permitted for a d^6 compound with an undistorted trigonal bipyramidal structure. Accordingly, $[\text{NEt}_4][\text{Fe}(\text{PS}_3^*)(\text{CO})]$ shows isotropically shifted resonances in the $^1\text{H NMR}$ ¹⁴ and a solid state magnetic susceptibility that are consistent with a paramagnetic ground state. A paramagnetic Fe(II)–CO complex has not been previously reported.¹⁷

We have recorded Mössbauer spectra of **2** from 4.2 to 200 K in applied fields up to 8.0 T. These spectra show that **2** is an integer spin paramagnet, and they impose axial symmetry on the spin Hamiltonian used in the simulations. This symmetry is in accord with the X-ray structure. The 4.2 K zero-field spectrum of Figure 3 exhibits a sharp quadrupole doublet¹⁸ with $\Delta E_Q = 2.31(2)$ mm/s and $\delta = 0.25(1)$ mm/s (relative to Fe metal at 298 K). The low value of δ rules out a high-spin ferrous site, whereas the observed paramagnetism is in conflict with a low-spin ferrous site. Thus, the data suggest a ground state with intermediate spin $S = 1$ for **2**. The Mössbauer spectra were simulated with the $S = 1$ spin Hamiltonian

$$H = D(S_z^2 - 2/3) + g\beta H \cdot S + S \cdot A \cdot I + 1/6 \Delta E_Q (3I_z^2 - 15/4) \quad (1)$$

for which $D = +30(6)$ cm^{-1} , $g_z = g_{\perp} = 2$,¹⁹ $A_{\perp} = -6.5$ MHz, $A_z = -48$ MHz, and $\Delta E_Q = -2.31$ mm/s. The negative sign of ΔE_Q suggests a concentration of negative charge along z , i.e., along the CO–Fe–P axis. Electronic structure calculations aimed at an interpretation of the fine and hyperfine structure parameters of **2** are in progress.

The lack of precedents for Ni(II)(CO) in model thiolate compounds has been a justification for discounting their existence in biological systems. This work suggests that CO coordination to a biological Ni(II) cysteine center must be considered as a viable possibility. This work also suggests that a Fe(II)(CO) center in a non-heme iron protein could be paramagnetic. The reactivity of these nickel and iron thiolate–carbonyl complexes are being investigated in an attempt to model the acetyl-CoA synthase function of CO dehydrogenase.

Acknowledgment. This research was supported by NIH Grant GM 31849 (S.A.K.), NIH Grant GM 36308 (M.M.), and NSF Grant MCB 9406274 (E.M.).

Supporting Information Available: Tables of crystallographic parameters, atomic coordinates, thermal parameters, and bond distances and angles for **1** and **2** (14 pages). See any current masthead page for ordering and Internet access instructions.

JA961968R

(17) Another example of a paramagnetic Fe(II)(CO) compound was published after this paper was submitted for publication. Ray, M.; Golombek, A. P.; Hendrich, M. P.; Young, V. G., Jr.; Borovik, A. S. *J. Am. Chem. Soc.* **1996**, 118, 6084.

(18) The spectrum of Figure 3 reveals a paramagnetic contaminant, amounting to 5% of total Fe.

(19) A magnetic susceptibility measurement of **2** at 298 K (sample of Figure 3) yielded a magnetic moment of 2.81 BM (different synthetic samples gave values of 2.81–2.85 BM). Taking into account the observed, but unidentified, impurity, a magnetic moment between 2.74 and 2.86 BM was obtained for **2**. This result confirms the $S = 1$ assignment for compound **2** and indicates that $g = 2$. For a given value of D , the low-temperature magnetic hyperfine interactions in the x – y plane are proportional to $g_{\perp}A_{\perp}/D$, while those along the z axis depend essentially on $g_z A_z e^{-D/kT}$; i.e., A , D , and g are strongly correlated.